Evidence for nonplanar atomic arrangement in graphite obtained by Raman spectroscopy

Yasushi Kawashima
Department of Mechanical Engineering, Faculty of Engineering, Tokai University, Hiratsuka, Kanagawa 259-1292, Japan

Gen Katagiri
Toray Research Center, Inc., Otsu, Shiga 520-8567, Japan

(Received 15 July 2002; published 30 September 2002)

It has been generally believed that graphite has a planar structure where atoms in the *A* site and the *B* site lie in the same plane without definite evidence. It is demonstrated that *A* and *B* atoms have different heights in the graphene layer on the basis of the observed Raman out-of-plane mode and mixed in-plane and out-of-plane modes by employing a lattice dynamic calculation and a double resonance mechanism. The crystal symmetry of graphite is a nonplanar C_{6v}^4 structure where the difference in height between *A* and *B* atoms is estimated to be about 0.2 Å.

DOI: 10.1103/PhysRevB.66.104109 PACS number(s): 78.30.Hv, 61.66.Bi, 78.30.Ly

Vibrational spectra of graphite have been well explained by the D_{6h}^4 space-group symmetry, so far,[1–6] assuming that the hexagonal networks of carbon atoms are stacked in an *ABABA* sequence and the *A* and *B* atoms have the same height from the basal plane of the unit cell. The zone-center modes assuming D_{6h}^4 structure are decomposed into the following irreducible representations: $\Gamma = A_{2u} + 2B_{2g} + E_{1u} + 2E_{2g}$. Only the two E_{2g} modes are Raman active. The A_{2u} and E_{1u} modes are infrared active and the B_{2g} modes are optically inactive. The A_{2u} and two B_{2g} modes have ''out-of-plane'' displacements while the E_{1u} and two E_{2g} modes are due to ''in-plane'' displacements. Graphite shows not only the E_{2g} bands but also several Raman bands arising from vibrational modes with nonzero wave vectors ($\mathbf{k} \neq 0$) in the first and higher-order regions.[1,2,6] Although these bands have been attributed to features in the density of states (DOS),[2] the laser excitation energy (E_L) dependence of several $\mathbf{k} \neq 0$ bands including the disorder-induced band around 1355 cm^{-1} (*D* band)[5,6] cannot be explained by the DOS model. Recently, the origin of the *D* band and its E_L dependence have been successfully elucidated by a double resonance process.[7] The *D* band has been assigned to phonons around *K* point belonging to the in-plane transverse optic (i-To) branch. Furthermore, this model has been extended to assign several other $\mathbf{k} \neq 0$ bands to phonons around Γ or *K* point which belong to the other branches.[8] However, there sill exist inexplicable features in the Raman spectrum of graphite.

The structure of graphite has been investigated by x-ray diffraction analysis. The results include that the atomic coordinates in each cell are at 0, 0, 0; 0, 0, 1/2 and 1/3, 2/3, *t*; 2/3, 1/3, $t+1/2$, where *t* cannot exceed 1/18.[9] Whether $t=0$ or $t \neq 0$, namely, planar or nonplanar structure of graphite, is difficult to discuss by the x-ray diffraction analysis because *t* can only be determined on the basis of the intensities of the reflections from the various planes and it will be very small even if $t \neq 0$. The space group of graphite with planar structure is D_{6h}^4 and that with the nonplanar structure is C_{6v}^4. Although the C_{6v}^4 space-group symmetry of graphite has been mentioned in the past,[10] evidence for the nonplanar structure has not been observed by vibrational spectroscopy, so far. The planar D_{6h}^4 structure has never contradicted the results previously obtained by Raman scattering, infrared spectroscopy, and inelastic neutron scattering. However, decisive evidence for the planar D_{6h}^4 structure has not also been given until now.

We have investigated closely the Raman scattering from various carbons ranging from highly graphitized to glassy materials employing excitation wavelength dependence and have found a number of Raman bands which had not been reported till then.[6] We have also found a distinct band at 867 cm^{-1} attributable to a zone-center mode with ''out-of-plane'' displacements in the Raman spectrum from the edge plane of highly oriented pyrolytic graphite (HOPG), which cannot be explained by the factor group analysis based on the planar D_{6h}^4 space group.[11]

We report the mixed in-plane and out-of-plane Raman bands of graphite which can be assigned to phonon modes around Γ or *K* point in terms of the double resonant Raman process.[7,8] On the basis of the lattice-dynamical calculation, we demonstrate that these bands should not appear on the assumption that graphite has the planar D_{6h}^4 structure. We propose the nonplanar $t \neq 0$ structure of graphite which successfully explains vibrational modes including the results obtained assuming the planar D_{6h}^4 structure. In addition, the difference in height between the *A* and *B* atoms of the nonplanar $t \neq 0$ structure is estimated from the effect of the double resonance condition that sensitively changes with the difference in height.

Raman spectra obtained from the HOPG edge plane with 514.5-nm-wavelength lights polarized parallel and perpendicular to the basal plane are shown in Figs. 1(a) and (b), respectively. In the first-order region of the spectrum Fig. 1(a), Raman bands are observed at 450, 650, 857, 1100, 1357, 1581, and 1621 cm^{-1}. The 450-, 650-, and 857-cm^{-1} bands are considered to be due to in-plane modes, because they cannot be clearly observed in the out-of-plane spectrum shown in Fig. 1(b). These bands are shown more clearly for glassy carbon (Tokai, GC30). The E_L dependences of the frequencies $[\delta(\Delta\nu)/\delta E_L]$ of the 450-, 650-, and 857-cm^{-1}

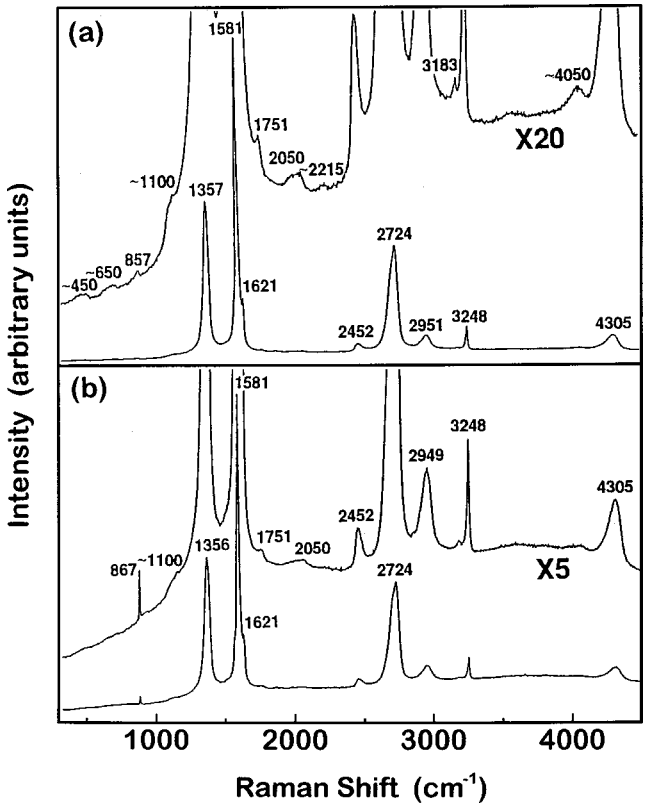

FIG. 1. Raman spectra from HOPG edge plane. (a) $E\|c$, (b) $E\perp c$.

bands as well as other fundamental bands are shown in Table I. Both the peak frequencies of the 450- and 650-cm^{-1} bands increase with increasing E_L, while the 857-cm^{-1} band does not vary much with E_L. According to the double resonance Raman scattering (DRRS) mechanism,[7,8] phonon modes satisfying the DRRS condition[8] can be observed due to drastic enhancement of the Raman scattering efficiency. The frequency of the DRRS band agrees with phonon energy at a point in the Brillouin zone (BZ) which meets the DRRS condition. The phonon energy can be obtained from the dispersion curves in terms of the manner described in Refs. 7 and 8. Furthermore, the sign and magnitude of $\delta(\Delta\nu)/\delta E_L$ for the band can be obtained from the slope of the dispersion curve to which the phonons belong. According to six phonon energy dispersion curves of two-dimensional (2D) graphite,

TABLE I. Peak positions, $\Delta\nu$ (cm^{-1}), the magnitude of the band shifts, $\delta(\Delta\nu)/\delta(E_L)$ (cm^{-1}/eV). (*) Determined on glassy carbon (Tokai, GC30).

$\Delta\nu$, (cm^{-1})	$\delta(\Delta\nu)/\delta E_L$, (cm^{-1}/eV)
450	168*
650	23*
857	−11*
1100	−62*
1357	50
1581	0
1621	0

TABLE II. The force-constant matrices for first-nearest three neighbors in the C_{6v}^4 and D_{6h}^4 structures. Here, $\phi_{\rm rto}^{(1)}=\phi_r^{(1)}\cos^2\varphi_1+\phi_{\rm to}^{(1)}\sin^2\varphi_1$, $\phi_{\rm tor}^{(1)}=\phi_{\rm to}^{(1)}\cos^2\varphi_1+\phi_r^{(1)}\sin^2\varphi_1$, $\phi_{\rm tr}^{(1)}=\frac{1}{2}(\phi_{\rm to}^{(1)}-\phi_r^{(1)})\sin 2\varphi_1$.

D_{6h}^4

$$\begin{pmatrix} \phi_r^{(1)} & 0 & 0 \\ 0 & \phi_{\rm ti}^{(1)}0 & \\ 0 & 0 & \phi_{\rm to}^{(1)} \end{pmatrix}$$

$$\begin{pmatrix} \frac{1}{4}\phi_r^{(1)}+\frac{3}{4}\phi_{\rm ti}^{(1)} & \mp\frac{\sqrt{3}}{4}(\phi_r^{(1)}-\phi_{\rm ti}^{(1)}) & 0 \\ \mp\frac{\sqrt{3}}{4}(\phi_r^{(1)}-\phi_{\rm ti}^{(1)}) & \frac{3}{4}\phi_r^{(1)}+\frac{1}{4}\phi_{\rm ti}^{(1)} & 0 \\ 0 & 0 & \phi_{\rm to}^{(1)} \end{pmatrix}$$

C_{6v}^4

$$\begin{pmatrix} \phi_{\rm rto}^{(1)} & 0 & \phi_{\rm tr}^{(1)} \\ 0 & \phi_{\rm ti}^{(1)} & 0 \\ \phi_{\rm tr}^{(1)} & 0 & \phi_{\rm tor}^{(1)} \end{pmatrix}$$

$$\begin{pmatrix} \frac{1}{4}\phi_{\rm rto}^{(1)}+\frac{3}{4}\phi_{\rm ti}^{(1)} & \mp\frac{\sqrt{3}}{4}(\phi_{\rm rto}^{(1)}-\phi_{\rm ti}^{(1)}) & -\frac{1}{2}\phi_{\rm tr}^{(1)} \\ \mp\frac{\sqrt{3}}{4}(\phi_{\rm rto}^{(1)}-\phi_{\rm ti}^{(1)}) & \frac{3}{4}\phi_{\rm rto}^{(1)}+\frac{1}{4}\phi_{\rm ti}^{(1)} & \pm\frac{\sqrt{3}}{2}\phi_{\rm tr}^{(1)} \\ -\frac{1}{2}\phi_{\rm tr}^{(1)} & \pm\frac{\sqrt{3}}{2}\phi_{\rm tr}^{(1)} & \phi_{\rm tor}^{(1)} \end{pmatrix}$$

the 450- and 857-cm^{-1} bands are assigned to phonon modes around Γ point which belong to the longitudinal acoustic (LA) and the out-of-plane transverse optic (o-TO) branches, respectively, and the 650-cm^{-1} band is attributed to phonon modes belonging to the o-TO branch around K point,[8,12] taking into account their Raman frequencies and excitation energy dependences. This indicate that the 450-cm^{-1} band is attributed to in-plane mode, while the 650- and 857-cm^{-1} bands are assigned to out-of-plane modes. The experimentally observed in-plane character of the 650- and 857-cm^{-1} bands is inconsistent with the assignments based on the dispersion curves for the D_{6h} planar structure.[12]

The 867-cm^{-1} band in Fig. 1(b) has been assigned to the zone-center mode with ''out-of-plane'' displacements.[11] The E_L dependence of the 867-cm^{-1} band cannot be distinguished within the accuracy of the experiment. This band is observed by light polarized with the electric vector parallel to the c axis which cannot excite the π states in the planar D_{6h}^4 structure.[13] The 867-cm^{-1} band cannot be explained by a double resonance process based on the assumption that graphite has the planar D_{6h}^4 structure.

The in-plane displacements of the 650- and 857-cm^{-1} modes indicate that there is a coupling between ''in-plane'' and ''out-of-plane'' vibrations in graphite lattice. Force-constant matrices for in-plane neighbors in the planar D_{6h}^4 structure are shown in Table II. The zx (xz) and yz (zy) elements of the force-constant matrices become zero, implying that intraplane interactions do not cause the mixed in-plane and out-of-plane modes. In the planar D_{6h}^4 structure, cou-

pling between vibrations parallel and perpendicular to the basal plane can arise only due to interplane interactions. We obtain the *zx* (*xz*) and *yz* (*zy*) elements of the dynamical matrix which are correlated to coupling between in-plane and out-of-plane vibrations, assuming the planar D_{6h}^4 structure of graphite. We first obtain the 12×12 dynamical matrix $D(\mathbf{k})$ for an arbitrary wave vector, $\mathbf{k}$, in the BZ, based on the Born–von Kármán model considering intraplane and interplane interactions up to fourth neighbor.[14] We express $\mathbf{k}$ using parameters u, v, and w $(0\leqslant u,\nu,w\leqslant 1)$ as

$$\mathbf{k}=\frac{1}{2}(\mathbf{b}_1+\mathbf{b}_2)u+\frac{1}{6}(\mathbf{b}_1-\mathbf{b}_2)u\nu+\frac{1}{2}\mathbf{b}_3 w, \tag{1}$$

where $\mathbf{b}_1$, $\mathbf{b}_2$, and $\mathbf{b}_3$ are the reciprocal basic vectors

$$\mathbf{b}_1=\frac{2\pi}{\sqrt{3}a_0}\hat{x}+\frac{2\pi}{a_0}\hat{y},$$

$$\mathbf{b}_2=\frac{2\pi}{\sqrt{3}a_0}\hat{x}-\frac{2\pi}{a_0}\hat{y},$$

$$\mathbf{b}_3=\frac{2\pi}{c_0}\hat{z}, \tag{2}$$

and $\hat{x},\hat{y},\hat{z}$ are unit vectors along the orthogonal axes [see Fig. 2(a)], and $a_0=2.46$ Å and $c_0=6.70$ Å are the lattice constants. In Eq. (1) the points $u=0$, $\nu=0$, $w=0$; $u=1$, $\nu=0$, $w=0$; and $u=1$, $\nu=1$, $w=0$ indicates Γ, M, and K points, respectively. Selecting only the *zx* or *yz* elements from each block $D_{\alpha\beta}$ $(\alpha,\beta=A,B,A',B')$ in the following dynamical matrix

$$D(\mathbf{k})=\begin{pmatrix} D_{AA} & D_{AB} & D_{AA'} & D_{AB'} \\ D_{BA} & D_{BB} & D_{BA'} & D_{BB'} \\ D_{A'A} & D_{A'B} & D_{A'A'} & D_{A'B'} \\ D_{B'A} & D_{B'B} & D_{B'A'} & D_{B'B'} \end{pmatrix}, \tag{3}$$

which is constructed using the site representation with four distinct *A*, *B*, *A'*, and *B'* atoms per unit cell,[15] for $\mathbf{k}$ in the BZ we have the 4×4 matrices D_{zx} and D_{yz}, respectively, composed of only the *zx* and *yz* elements

$$D_{xz}(\mathbf{k})=\begin{pmatrix} 0 & 0 & \gamma & \alpha i e^{(1/3)i\pi u} \\ 0 & 0 & \alpha i e^{(1/3)i\pi u} & -\alpha i e^{-(1/3)i\pi u} \\ \gamma & -\alpha i e^{-(1/3)i\pi u} & 0 & 0 \\ -\alpha i e^{-(1/3)i\pi u} & \alpha i e^{(1/3)i\pi u} & 0 & 0 \end{pmatrix}, \tag{4}$$

$$D_{yz}(\mathbf{k})=\begin{pmatrix} 0 & 0 & \delta & \beta e^{(1/3)i\pi u} \\ 0 & 0 & \beta e^{(1/3)i\pi u} & \beta e^{-(1/3)i\pi u} \\ \delta & \beta e^{-(1/3)i\pi u} & 0 & 0 \\ \beta e^{-(1/3)i\pi u} & \beta e^{(1/3)i\pi u} & 0 & 0 \end{pmatrix}, \tag{5}$$

where α, β, and γ are given by

$$\alpha=\sin\left(\frac{1}{2}\pi w\right)\left[(\hat{\phi}_r^{(2)}-\hat{\phi}_t^{(2)})\sin 2\phi_1\left\{1+\cos\left(\frac{1}{3}\pi u\nu\right)\right\}\right.$$
$$\left.-(\hat{\phi}_r^{(4)}-\hat{\phi}_t^{(4)})\sin 2\phi_3\left\{1-\cos\left(\frac{2}{3}\pi u\nu\right)\right\}\right],$$
$$\beta=-\sqrt{3}\sin\left(\frac{1}{2}\pi w\right)\left\{(\hat{\phi}_r^{(2)}-\hat{\phi}_t^{(2)})\sin 2\phi_1\sin\left(\frac{1}{3}\pi u\nu\right)\right.$$
$$\left.-(\hat{\phi}_r^{(4)}-\hat{\phi}_t^{(4)})\sin 2\phi_3\sin\left(\frac{2}{3}\pi u\nu\right)\right\},$$
$$\gamma=-2\sqrt{3}(\hat{\phi}_r^{(3)}-\hat{\phi}_t^{(3)})\sin 2\phi_2$$
$$\times\sin\left(\frac{1}{2}\pi w\right)\sin(\pi u)\cos(\tfrac{1}{3}\pi u\nu),$$
$$\delta=-2(\hat{\phi}_r^{(3)}-\hat{\phi}_t^{(3)})\sin 2\phi_2\sin\left(\frac{1}{2}\pi w\right)$$
$$\times\left\{\cos(\pi u)\sin\left(\frac{1}{3}\pi u\nu\right)+\sin\left(\frac{2}{3}\pi u\nu\right)\right\}. \tag{6}$$

In Eq. (6), $\hat{\phi}_r^{(n)}$ and $\hat{\phi}_t^{(n)}$ represent the radial and tangential force constants for interaction between the nth out-of-plane nearest neighbors, respectively,[14] and ϕ_1, ϕ_2, ϕ_3 are shown in Fig. 2(a). Putting $w=0$ in Eqs. (4) and (5), we find that both the D_{zx} and D_{yz} become zero. This implies that no coupling between vibrations parallel and perpendicular to the basal plane takes place at any point in the ΓMK plane, because the effects of the interplane interactions cancel due to the *ABABA* stacked structure. Phonon mode at a point away from the ΓMK plane does not satisfy the wave-vector conservation relation concerning the *c*-axis direction. Therefore, the phonon that can give rise to first-order Raman scattering is limited to the ΓMK plane. The effect of coupling between in-plane and out-of-plane vibrations cannot appear in the Raman spectrum of the D_{6h}^4 planar structure.

The observation of the 650- and 857-cm^{-1} bands shows that coupling between in-plane and out-of-plane vibrations results from atomic interactions within a graphene layer, not from interlayer interactions.

In order to explain the strong coupling, we construct a nonplanar structure slightly deviated from the D_{6h}^4 structure

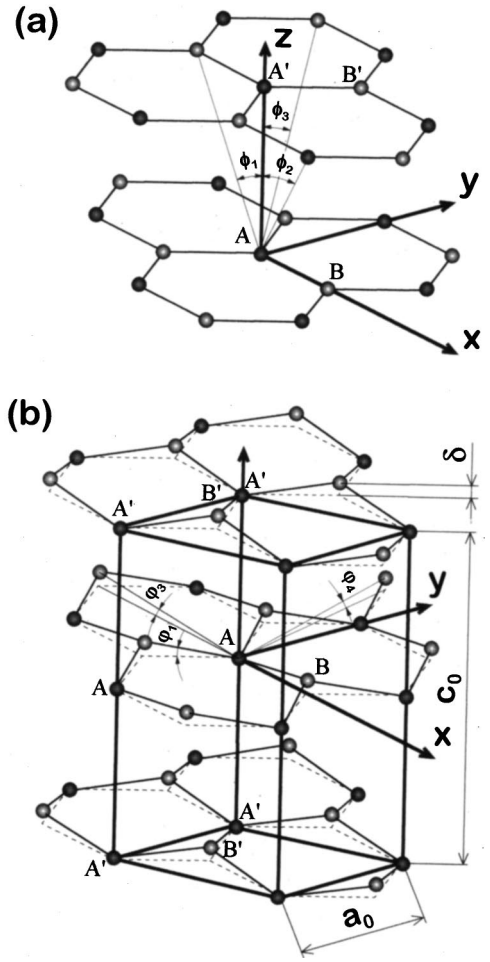

FIG. 2. (a) Structure of graphite with D_{6h}^4 space-group symmetry. (b) Structure deviated from planar structure of graphite with C_{6v}^4 space-group symmetry. The broken lines indicate the honeycomb lattice of D_{6h}^4 space group.

to satisfy the geometries of graphite structure determined by x-ray measurements,[9] where in each cell the A and B (A' and B') atoms do not have the same height above the basal plane of the cell and the difference in height between the A and B atoms is equal to that of the A' and B' atoms. The structure, which belongs to the space group C_{6v}^4, is shown in Fig. 2(b). In this structure the force-constant matrices for first neighbors have nonzero zx (xz) and yz (zy) elements as listed in Table II and the first-neighbor interactions cause strong coupling between ''in-plane'' and ''out-of-plane'' vibrations. We consider only lattice vibrations in a single layer, since the effect of interlayer interactions can be ignored as compared with the interactions within the layer. This 2D model is also applicable to glassy carbon which shows the 650- and 857-cm^{-1} bands more clearly.

We also obtain the 6×6 dynamical matrix D for one layer of the C_{6v}^4 structure in the same manner as the D_{6h}^4 structure. The 2×2 matrices D_{zx} and D_{yz} are constructed separately from the dynamical matrix as follows:

$$D_{xz}=\begin{pmatrix} 0 & \alpha' e^{-(1/3)i\pi u} \\ \alpha' e^{(1/3)i\pi u} & 0 \end{pmatrix},$$

$$D_{yz}=\begin{pmatrix} 0 & \beta' i e^{-(1/3)i\pi u} \\ -\beta' i e^{(1/3)i\pi u} & 0 \end{pmatrix}, \tag{7}$$

where α' and β' are given by

$$\alpha'=\phi_{\rm tr}^{(1)}\left\{1+\cos\left(\frac{1}{3}\pi u\nu\right)\right\}-\phi_{\rm tr}^{(3)}\left\{1-\cos\left(\frac{2}{3}\pi u\nu\right)\right\}$$
$$-\frac{1}{\sqrt{7}}\phi_{\rm tr}^{(4)}\left\{5\cos\left(\frac{1}{3}\pi u\nu\right)-\cos(\pi u\nu)+4\cos\left(\frac{2}{3}\pi u\nu\right)\right\},$$

$$\beta'=-\sqrt{3}\left[\phi_{\rm tr}^{(1)}\sin\left(\frac{1}{3}\pi u\nu\right)-\phi_{\rm tr}^{(3)}\sin\left(\frac{2}{3}\pi u\nu\right)\right.$$
$$\left.+\frac{1}{\sqrt{7}}\phi_{\rm tr}^{(4)}\left\{\sin\left(\frac{1}{3}\pi u\nu\right)+3\sin(\pi u\nu)-2\sin\left(\frac{2}{3}\pi u\nu\right)\right\}\right]. \tag{8}$$

In Eq. (8) $\phi_{\rm tr}^{(n)}=\frac{1}{2}(\phi_{\rm to}^{(n)}-\phi_r^{(n)})\sin 2\varphi_n$, the $\phi_r^{(n)}$ and $\phi_{\rm to}^{(n)}$ represent the radial and out-of-plane tangential force constants between nth nearest neighbors,[12] and φ_1, φ_3, φ_4 are illustrated in Fig. 2(b). The terms α' and β' increase as the difference in height between A and B (δ) increases. While β' becomes zero along the line from Γ to M point ($v=0$), α' is not zero at any point in the BZ. This indicates that all phonon modes have both the in-plane and out-of-plane displacements in the C_{6v}^4 structure.

We calculate the dispersion curves for the single layer structure with various difference in height ($t=\delta/c_0$) ranging from 0 to 1/18 using the same 12 force constants as those listed in Ref. 12. The phonon dispersion curves in the case of $t=1/36$ are shown in Fig. 3(a) where data points of the 450-, 650-, 857-, and 1356-cm^{-1} bands observed with 514.5-nm excitation are denoted according to the DRRS mechanism. Figure 3(a) shows that the dispersion curves do not intersect at $0.52\mathbf{k}_M$ differently from those of planar D_{6h} structure, where $\mathbf{k}_M$ is the wave vector of the M point. The distance at $0.52\mathbf{k}_M$ between the two dispersion curves showing the apparent crossing in the D_{6h} structure results from coupling between in-plane and out-of-plane vibrations which increases as t increases. Changing t from 1/72 to 1/18, the ratios of the amplitude of vibration within the x-y plane to that of vibration along the z axis for the 650- and 857- cm^{-1} phonon modes increase from 0.046 and 0.042 to 0.15 and 0.12, respectively. In the nonplanar structure, it is confirmed that the phonon modes have sufficient in-plane displacements to cause observable Raman peaks by a double resonance process.

The electronic energy dispersion relations for the nonplanar 2D graphite where $t=1/36$ is shown in Fig. 3(b), which are calculated by the tight-binding method using the same parameters as listed in Ref. 16. As seen from Fig. 3(b), phonons for which double resonance occurs in the nonplanar C_{6v} structure should be located at a longer distance from Γ or K point as compared to those in the case of the planar D_{6h} structure. Plots of Raman observations based on the DRRS mechanism assuming the planar D_{6h} structure and the non-

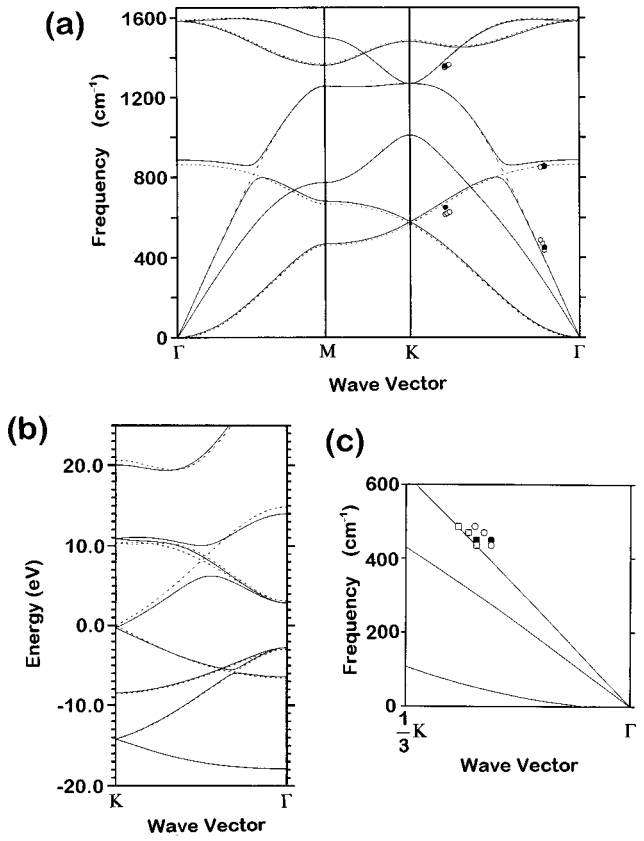

FIG. 3. (a) Calculated phonon dispersion curves for the planar D_{6h} (dotted line) and the nonplanar structure with $t=1/36$ (solid line). Experimental Raman observations based on the DRRS model are also shown, "●" (HOPG); "○" (GC30). (b) Calculated electronic energy dispersion curves for the nonplanar 2D graphite in the case that $t=1/36$. Dotted line indicates the electronic energy dispersion curves for the planar D_{6h} structure. (c) Comparison of plots based on the planar D_{6h} structure and the nonplanar C_{6v} structure under the application of the DRRS mechanism. "●, ○"—the planar D_{6h} structure; "■, □"—the nonplanar C_{6v} structure with $t=1/36$. "●, ■" (HOPG); "○, □" (GC30).

planar C_{6v} structure are shown in Fig. 3(c), where the phonon dispersion curves were calculated to fit the experimental data.[17–19] Figure 3(c) shows that plots assuming the D_{6h} structure deviate from the dispersion curve. The plots of the nonplanar structure with $t=1/36$ lie almost within the dispersion curve, indicating that a difference in height between *A* and *B* atoms can be estimated to be about 0.2 Å. Although the difference in height between *A* and *B* atoms may also be obtained from the dispersion curves measured by electron-energy-loss spectroscopy (EELS) experiments,[18] the small distance between the dispersion curves at $0.52\mathbf{k}_M$ will be difficult to distinguish by EELS measurements because of its low energy resolution.

TABLE III. The correlation of the zone-center modes of C_{6v}^4 and D_{6h}^4 crystal structures. Raman and infrared activity is indicated in the parentheses by *R* and IR, respectively.

D_{6h}^4	A_{2u} (IR)	B_{2g}	E_{1u} (IR)	$E_{2g}(R)$
C_{6v}^4	$A_1(R,\mathrm{IR})$	B_1	$E_1(R,\mathrm{IR})$	$E_2(R)$

Let us consider now whether other vibrational modes previously observed are consistent with the proposed nonplanar C_{6v}^4 structure. The zone-center modes according to the factor group analysis based on C_{6v}^4 can be decomposed into the following irreducible representations: $\Gamma=A_1+2B_1+E_1+2E_2$. The vibrations of A_1 and two B_1 species constitute out-of-plane modes while those of E_1 and two E_2 species are the in-plane modes. The correlation between the irreducible representations of modes for C_{6v}^4 and D_{6h}^4 is given in Table III, in which the Raman and infrared active modes are also identified. As seen from Table III, the A_1 and E_1 (C_{6v}^4) modes are infrared and Raman active whereas the A_{2u} and E_{1u} (D_{6h}^4) modes are infrared active and Raman inactive. The frequency of the out-of-plane infrared active mode identified by infrared spectroscopy[20] agrees with that of the out-of-plane mode at 867 cm^{-1} observed in the Raman spectrum from HOPG edge plane,[11] implying that the 867-cm^{-1} mode can be assigned to the Raman and infrared active A_1 mode. The Raman E_1 peak will be observed at a position very close to the E_2 (C_{6v}^4) band (1581 cm^{-1}).[20] As a result, the optical properties of the zone-center modes previously observed for graphite can be well explained by C_{6v}^4.

We demonstrate that the bands due to mixed "in-plane" and "out-of-plane" modes arise from the nonplanar C_{6v}^4 structure of graphite. The difference in height between *A* and *B* atoms can be estimated to be about 0.2 Å in terms of the DRRS mechanism. According to the C_{6v}^4 structure, all the zone-center modes including the Raman active out-of-plane 867-cm^{-1}mode can be successfully explained. In conclusion, we propose the nonplanar C_{6v}^4 structure for graphite which is compatible with the results of vibrational and x-ray measurements obtained so far.

We thank K. Okada and Y. Takahashi of Toray Research Center, Inc. for their comments.

[1] F. Tuinstra and J. L. Koenig, J. Chem. Phys. **53**, 1126 (1970).
[2] R. J. Nemanich and S. A. Solin, Phys. Rev. B **20**, 392 (1979).
[3] L. J. Brillson, E. Burstein, A. A. Maradudin, and T. Stark, in *Physics of Semimetals and Narrow-Gap Semiconductors*, edited by D. L. Carter and R. T. Bate (Pergamon, New York, 1971), p. 187.
[4] R. Nicklow, N. Wakabayashi, and H. G. Smith, Phys. Rev. B **5**, 4951 (1972).
[5] R. P. Vidano, D. B. Fischbach, L. J. Willis, and T. M. Loehr, Solid State Commun. **39**, 341 (1981).
[6] Y. Kawashima and G. Katagiri, Phys. Rev. B **52**, 10 053 (1995).
[7] C. Thomsen and S. Reich, Phys. Rev. Lett. **85**, 5214 (2000).
[8] R. Saito, A. Jorio, A. G. Souza Filho, G. Dresselhaus, M. S. Dresselhaus, and M. A. Pimenta, Phys. Rev. Lett. **88**, 027401

(2002).
[9] J. D. Bernal, Proc. R. Soc. London, Ser. A **106**, 749 (1924).
[10] W. G. Wyckoff, *Crystal Structures* (Interscience Publishers, Inc., New York, 1960), Vol. I, p. 26.
[11] Y. Kawashima and G. Katagiri, Phys. Rev. B **59**, 62 (1999).
[12] M. S. Dresselhaus and P. C. Eklund, Adv. Phys. **49**, 705 (2000).
[13] D. L. Greenaway, G. Harbeke, F. Bassani, and E. Tosatti, Phys. Rev. **178**, 1340 (1969).
[14] R. Al-Jishi and G. Dresselhaus, Phys. Rev. B **26**, 4514 (1982).
[15] S. Y. Leung, G. Dresselhaus, and M. S. Dresselhaus, Phys. Rev. B **24**, 6083 (1981).
[16] R. Saito, G. Dresselhaus, and M. S. Dresselhaus, *Physical Properties of Carbon Nanotubes* (Imperial College Press, London, 1998).
[17] R. A. Jishi, L. Venkataraman, M. S. Dresselhaus, and G. Dresselhaus, Chem. Phys. Lett. **209**, 77 (1993).
[18] C. Oshima, T. Aizawa, R. Souda, Y. Ishizawa, and Y. Sumiyoshi, Solid State Commun. **65**, 1601 (1988).
[19] T. Aizawa, R. Souda, S. Otani, Y. Ishizawa, and C. Oshima, Phys. Rev. B **42**, 11 469 (1990).
[20] R. J. Nemanich, G. Lucovsky, and S. A. Solin, Solid State Commun. **23**, 117 (1977).